

## System Design for Passive Human Detection using Principal Components of the Signal Strength Space

Bojan Mrazovac<sup>1</sup>, Milan Z. Bjelica<sup>1</sup>, Dragan Kukolj<sup>1</sup>, Branislav M. Todorović<sup>2</sup> and Saša Vukosavljev<sup>2</sup>

<sup>1</sup> Faculty of Technical Sciences, Trg Dositeja Obradovića 6,  
21000 Novi Sad, Serbia

{bojan.mrazovac, milan.bjelica, dragan.kukolj}@rt-rk.com

<sup>2</sup> RT-RK, Institute for Computer Based Systems, Narodnog Fronta 23a,  
21000 Novi Sad, Serbia

{branislav.todorovic, sasa.vukosavljev}@rt-rk.com

**Abstract.** In this article, device-free human presence detection method based on principal components analysis of the radio signal strength variations is proposed. The method increases user awareness for automated power management interaction in residential power saving systems. Motivation comes from a need for decreasing the installation complexity and development costs induced by the integration of specific human presence detection sensors. The method exploits the fact that a human body interferes with radio signals by introducing irregularities in the radio signature which indicate possible human presence. By analyzing radio signals between radio transceivers embedded in 2.4 GHz wireless power outlets, the original environment is not visually modified and a certain level of sensorial intelligence is introduced without additional sensors. The analysis of the signal strength variations in principal components space enhances the detection accuracy level of human presence detection method, retaining low installation costs and improving overall energy conservation.

**Keywords:** energy awareness, human presence detection, principal components analysis, radio irregularity, RSSI, smart outlets, Zigbee.

### 1. Introduction

Due to the rise of the global energy demands, the electricity price increase and the limitation of natural resources used for electricity generation, several considerations about the energy saving have been brought up recently [1], [2], [3], [4], [5]. An optimized approach for residential electric energy conservation requires installation of power metering devices. The European Union and the European Regulators' Group for Electricity and Gas have proposed an initiative [6] to encourage the installation of smart power meters

in all homes across Europe during the next decade. The most frequently used solution for smart power metering is made in a form of smart power outlets. Smart outlets offer the possibility for additional energy-related services such as on-demand power management, overview of the consumed energy and power switching of plugged devices. Such an approach provides more accessible information which help people to use energy more efficiently.

Although consumers are aware about their power consumption, their habits are very difficult to change and in many cases no corrective actions that would decrease the power consumption are taken. Therefore, there exists a need for automated power management solution, which does not require a user to intervene. To enable the automatic response, it is necessary to establish the interaction with the environment by integrating a number of sensors, mainly for human presence detection. An example of interactive energy saving platform is proposed in the previous work as "*Ecosystem for Smart Home*" (ESH) [5]. The ESH improves the power consumption efficiency by connecting smart power outlets and smart light switches, which are part of pre-existing electrical installations, with human presence detection sensors. The integration of sensors and smart power nodes increases user awareness of the smart home for the advanced automated power management.

Human presence detection method, proposed in this article, is motivated by a need for decreasing the installation complexity and development costs induced by the integration of specific sensors in smart energy environment. As opposed to the original ESH framework which incorporates various human presence detection sensors, the proposed method detects human presence without specific sensors. The detection is enabled only by analyzing and quantifying radio signal strength variations at the inputs of radio transceivers embedded in wireless nodes. This approach exploits the fact that human bodies interfere with radio signals, causing fading and shadowing effects. Therefore, irregularities in the radio signature, given in a form of received signal strength indicator's (RSSI) variations, are considered as an indication of possible presence in the room. The method extracts principal components from a covariance matrix composed of samples that present signal strengths gathered from wireless links inside a room. Principal component analysis enhances the accuracy level with small percentage of false alarms and improves the overall probability of human presence detection. Since the most of indoor environments contain power outlets, replacing them with smart power outlets would not modify the environment visually, but existing electrical installations would be extended with the detection capability. The use of radio irregularity from radio links in an already installed network of wireless power outlets preserves the transparency of smart home devices, supports high level of sensorial intelligence and has low installation cost.

The paper is structured as follows. In Section 2, an overview of device-free methods for human presence detection is given, including theoretical background. In addition, an overview of smart energy systems for residential use is introduced. The proposed human presence detection method is explained in Section 3. The ESH system which incorporates the proposed

method is described in Section 4. Experimental results are given in Section 5. At the end of the paper, in Section 6, a conclusion with an idea for the future improvement is given.

## 2. Related Work and Theoretical Framework

Radio irregularity is a common phenomenon which is often considered as a shortcoming of radio networks. A number of experiments set in [7] and [8] explain that radio irregularity is mainly caused by two factors: device properties and the propagation medium. Device properties include: the antenna type, the transmitter's radiated power, the receiver's sensitivity, and signal-to-noise ratio. Medium properties include the background noise and the environmental factors such as obstacles within the propagation path. When the signal travels through a medium, it may be absorbed, scattered, reflected or diffracted. At microwave frequencies, absorption by molecular resonance is a major factor affecting the radio propagation [9]. Scattering occurs when the signal propagates through a medium which contains a large number of objects smaller than the signal's wavelength. Reflection occurs when the signal encounters an object which is larger than the signal's wavelength. Diffraction occurs when the signal encounters an irregular surface, such as sharp edges.

The irregularity of the radio signals is even more expressed when a human body encounters the signal in its propagation path. The human body is comprised of molecules of water which are able to additionally absorb, diffract, scatter or reflect the energy of the radio signal. Therefore, the presence of a human within the wireless network range results in significant signal strength variations at the receiver, whereas the degree of the signal strength variation is correlated with the level of human motion.

Woyach *et al.* [10] report that the shadowing effect caused by a human subject moving in the line-of-sight path between two communicating wireless nodes can be used for human motion detection. Such an approach, mainly based on RSSI variations analysis is extended for the outdoor people counting mechanism [11]. Lee *et al.* [12] investigated the feasibility of intrusion detection by characterizing the signal strength fluctuations and translating them into sufficient information that corresponds to an intruder's activity. The presented idea is extended for an indoor automated people counting mechanism [13]. Intruder detection method [14] enabled by exploiting RSSI considerations, confirms the hypothesis that irregularities in the RSSI signature can be used as human presence indication. Through distributed processing of RSSI samples, nodes deployed in an indoor environment can also detect human presence and possibly help in localizing and tracking moving individuals, as shown by Kaltiokallio *et al.* [15]. The use of RSSI variations due to radio irregularity for security threats detection alongside a roadway, explained by Puzo *et al.* [16], demonstrates the ability of passive wireless sensor networks (PWSN) to be applied for the outdoor

surveillance. Patwari and Wilson [17] explain how multi-path fading can be used for the benefit of device-free localization systems. In such environments denoted as “RF sensor networks”, a human position can be inferred by measuring the absorption, reflection, scattering and diffraction of an electromagnetic wave, intersected by the human body. Device-free human localization in indoor environments using “RF sensor networks” is also the topic of the research presented by Deak *et al.* [18]. The phrase “RF sensor network” comes from the fact that the wireless network itself is the sensor, using RF signals to probe the environment. It is important to mention that a human does not need to be carrying a wireless device to be detected. Zhang *et al.* [19] proposed an RF sensor network operating at 870 MHz for indoor people tracking. The positioning method is based on capturing the RSSI dynamics of the reflected signals, which varies due to subject movement. That approach is further extended in [20] to implement the system capable of multiple persons tracking, simultaneously moving in the monitored area. The algorithm is based on distributed dynamic clustering that improves the localization accuracy when multiple subjects are present. Moussa and Youssef [21] demonstrate the feasibility of device-free passive intruder detection and localization by using the moving average of RSSI variance to detect the intrusion events.

The most of the existing residential smart energy solutions have one important attribute in common: they rely on various sensor technologies and sensor networks, such as [1], [2], [5], [22], [23], [24], [25], [26]. Because of the important impact of sensor networks applications in smart home’s environmental challenges, the authors of this paper have tried to make a synthesis between “RF sensor networks” and residential smart energy systems. In order to detect human presence in smart energy infrastructure, an algorithm that characterizes the signal strength variations, has been previously proposed in [27] and [28]. The algorithm is incorporated into the smart power outlets, by enabling them to detect human presence only by analyzing and quantifying radio signal strength variations incorporated in exchanged messages. The RSSI standard deviation and discrepancies between the mean value of a set of RSSI samples and the set’s min and max values are compared to define the interval of the initial signal strength variation. During the runtime, each outlet is polled periodically by the specific controller device, to obtain their current RSSI values from the messages exchanged with other outlets. The algorithm compares read RSSI values with the interval’s bounds. When the human steps into the monitoring area, the signal strength variation exceeds the previously set bounds and reports the presence of a subject. The shortcoming of such an approach is that the algorithm monitors RSSI variation intensity on each link independently. It is enough that the interval is exceeded only at one link and the detection will be reported. This is also the case for many related researches that were performed in a controlled environment. Unfortunately, in real environment, the external noise (e.g. interferences from another room, or single link variations for specific positions in the room) can disturb a radio link in the monitoring room, resulting in reported false alarms.

In order to improve the presence detection for real-world applications, the RSSI processing algorithm resistant to external noise is proposed in this paper. To meet the requirement, the authors propose the use of Principal Components Analysis (PCA). The RSSI variation intensity is given as a function over the entire network of radio links (RSSI) in the monitoring room. The links are simultaneously processed, therefore in a case when a few links are interfered with the external noise, the power of the majority of links will minimize, or even entirely suppress the noise. PCA successfully filters out the disturbed signals in order to preserve the correct detection.

### 3. Human Presence Detection Method based on Principal Components Analysis of the Signal Strength

Principal components analysis [29], [30] is a useful statistical technique used in many forms of statistical analysis, from biomedical signal processing [31] to computer graphics and pattern recognition [32]. It presents a simple, non-parametric method for extracting relevant information from confusing and large data sets. PCA is a variable reduction procedure. It is useful when samples are obtained on a large number of variables that are mutually correlated. PCA helps identifying patterns in the data, and expressing the data in a way that highlights their similarities or differences. Because of this variables redundancy, it is possible to reduce the large set of observed variables into a smaller number of principal components while retaining as much as possible of the variation present in the original data set. As the final result, each principal component contains new information about the original data and is ordered so that the first few components account for most of the variability. In the proposed algorithm, PCA compresses raw RSSI inputs obtained from each radio link, in order to extract principal components that are used to emphasize the variability of the signal strength.

A set of RSSI samples obtained from a communication link between two wireless nodes (outlets) inside the same room forms the zero-mean column vector  $linkToNod_k$ :

$$linkToNod_k = \begin{bmatrix} sample(1) \\ sample(2) \\ \dots \\ sample(N) \end{bmatrix}. \quad (1)$$

Vector  $linkToNod_k$  stores the information about RSSI signature from the link between a node which is currently polled by the home controller, and another node which communicates with the polled node. Each value  $sample(i)$  denotes an RSSI sample obtained from that link, whereas the counter  $i$  takes its values from 1 to  $N$ , for  $N$  that is the number of samples in the observed time window. Counter  $k$  takes its values from 1 to  $K-1$ , where  $K$

represents the number of all active nodes inside the detection scope. Links toward remaining nodes represent an ensemble of  $K-1$  sensing links. The entire ensemble can be compactly expressed by the  $N \times (K-1)$  data matrix  $Nod$ , which defines  $(K-1)$  observations of the random process:

$$Nod = [linkToNod_1 \quad linkToNod_2 \quad \dots \quad linkToNod_{k-1}] \quad (2)$$

Once the samples are collected, the shift interval which includes number of  $p$  samples from each column of matrix  $Nod$  needs to be defined. Over new set of  $p$  samples, the standard deviation (STD) is calculated. The interval of first  $p$  samples is further represented through the value  $stdLink_p$ , which shows the standard deviation of the vector  $p$  calculated over a single link. Afterwards, the STD is performed for the rest of the columns of matrix  $Nod$  which contain the data from other active links. That way, the shifting interval and the STD calculation applied to  $p$  samples from each column can be saved in a new vector  $z_k$ :

$$z_k = [stdLink_1 \quad stdLink_2 \quad \dots \quad stdLink_{k-1}] \quad (3)$$

The procedure for the creation of the vector  $z_k$  is repeated for each  $K$ -th node, after the node is polled by the home controller. Counter  $k$  denotes the id of the polled node and takes its values from 1 to  $K$ , where  $K$  is the number of nodes in the environment. The calculated values are stored into new  $(K-1) \times K$  matrix  $X$ :

$$X = [z_1 \quad z_2 \quad \dots \quad z_K] \quad (4)$$

whose columns represent transposed vectors  $z_k$ , for each wireless node. After the samples are collected it is important to determine how much the dimensions vary from the mean value with respect to each other. For that purpose the statistical measure covariance ( $cov$ ) is used:

$$cov(z_i, z_j) = \frac{\sum_{s=1}^{K-1} (z_i(s) - \bar{z}_i)(z_j(s) - \bar{z}_j)}{((K-1)-1)} \quad (5)$$

$$i, j = [1, K] \wedge i \neq j \quad ,$$

where  $\bar{z}_i$  and  $\bar{z}_j$  denote mean values from the set of samples per vectors  $z_i$  and  $z_j$ , respectively:

$$\bar{z}_i = \frac{1}{K-1} \sum_{s=1}^{K-1} z_i(s), \quad \bar{z}_j = \frac{1}{K-1} \sum_{s=1}^{K-1} z_j(s) \quad (6)$$

The expression (5) is divided by  $(K-1)-1$ , because the data represent only a sample. This gives the result that is closer to the standard deviation, which would result if the entire population is used. As the next step of the algorithm, all the possible covariance values between the variables should be calculated

and stored into covariance matrix  $C_X$ . By using the equation (4) that defines the matrix of links  $X$ , the covariance matrix can be expressed as:

$$C_X = \frac{1}{(K-1)-1} XX^T . \quad (7)$$

Each row of  $X$  corresponds to all measurements of a particular link. Each column of  $X$  corresponds to a set of measurements from one particular polling cycle. The matrix  $C_X$  captures correlations between all the possible pairs of measurements. A large value of  $C_X$  indicates high redundancy between measurements, whereas small indicates low redundancy.

PCA enables the linear transformation that maps the data from a higher dimensional space to a lower dimensional space. Low dimensional space is determined by the strongest eigenvectors of the covariance matrix  $C_X$ , known as principal components. The eigenvectors of  $C_X$  are non-zero vectors that, after being multiplied by the matrix  $C_X$  remain proportional to the original vector or become zero. An eigenvalue represents the scalar which defines how the eigenvector changes (stretches, flips, shrinks or leaves unchanged) when it gets multiplied by matrix  $C_X$ .

If  $W$  is a vector space and  $w$  is a vector from that space, then  $w$  represents an eigenvector of matrix  $C_X$  with eigenvalue  $\lambda$ , defined as:

$$C_X w = \lambda w . \quad (8)$$

The eigenvalues of  $C_X$  can be calculated as the roots of characteristic polynomial which can be derived from the expression:

$$\det(C_X - \lambda I) = 0 , \quad (9)$$

where  $\det$  stands for determinant and  $I$  is the  $K \times K$  identity matrix. The eigenvectors correspond to principal components whereas the eigenvalues correspond to the variance defined by the principal components. Once the eigenvectors are found from the covariance matrix  $C_X$ , the next step is to order them by eigenvalues, highest to lowest, which orders the principal components by their significance. By ignoring less significant components, the final data set will have less dimensions than the original. The last step of the algorithm is to form the *Feature Vector*  $fv$  which is constructed by using the most significant eigenvalues. By analyzing the eigenvalues saved in the vector  $fv$ , the presence of a human can be determined. No presence implicates very low RSSI variations and therefore low eigenvalues (very close to value 0). When a human subject is present, RSSI variations from wireless links are becoming higher, with strongly expressed deviations from the mean value, which implicates higher eigenvalues. The detection bound is set to be the maximal value from the  $fv$  during the phase of training (no humans in the room). During the runtime, the eigenvalues which are higher

than the bound, report human presence. Lower eigenvalues report the empty room.

#### 4. Case Study – System Design for Residential Energy Awareness

In one of the previous papers a smart energy system for the residential use has been presented [5]. The system is comprised of the home controller device, 2.4GHz (*IEEE 802.15.4*) wireless smart outlets, 2.4GHz smart light switches and a number of residential sensors. All these devices are connected to the residential smart power network. By interpreting user-defined power saving schemes given in a form of XML based scripts [33] the user awareness of the entire system is increased. Increased awareness enables automation of instructions that generate ambient intelligence environment. The concept is depicted in Fig.1.

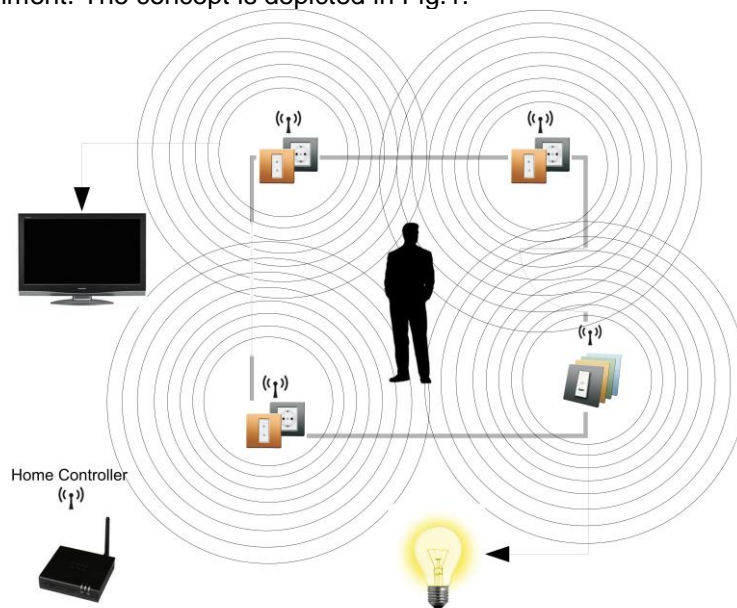


**Fig. 1.** The concept of human presence detection method based on wireless smart outlets, light switches and the analysis of RSSI variations

Implementation of the proposed method for presence detection requires at least two smart wireless power outlets, which can be combined with smart light switches. The communication control, periodic polling mechanism and the RSSI data analysis are implemented within the core software modules of the home controller. The home controller (illustrated in Fig. 2) is made in a form of a software platform based on POSIX/C open standards which provide

## System Design for Passive Human Detection using Principal Components of the Signal Strength Space

scalability. The software is platform independent and can be easily ported to various POSIX-based target controllers.

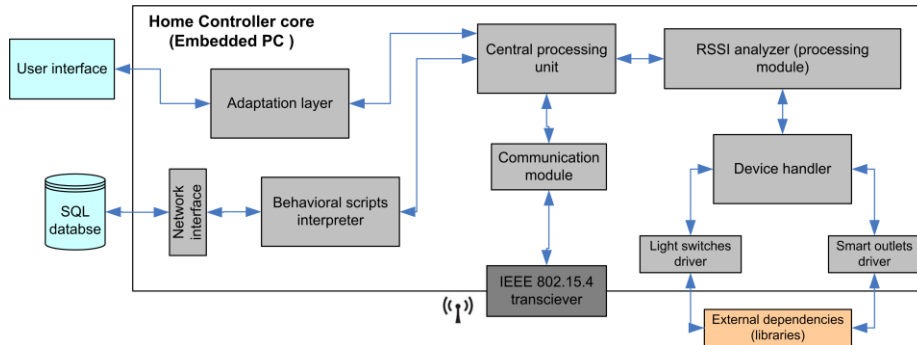


**Fig. 2.** The home controller software design. The home controller is comprised of adaptation layer which provides communication toward user interface; RSSI analyzer which polls each outlet and analyzes RSSI data; the communication module which provides communication with the smart wireless nodes and user interfaces; the device handler which provides device drivers for smart nodes; and the behavioral scripts interpreter which provides engine for user-defined power saving schemes execution

The device handler module connects device drivers for smart outlets and light switches with the central processing unit, providing a communication mechanism for wireless nodes polling and RSSI data reading. The device handler controls the message flow as the response on detection events. The RSSI analyzer enables periodic polling of wireless nodes to retrieve the current values of RSSI. The home controller polls each node (outlet) in turn on every 100ms and saves the received values in the local storage database. That way the system is able to detect even a human running with the fastest known speed without unnecessary frequent polling that can bring high processing loads to the system.

Once a node receives the polling command from the home controller it sends its RSSI table as a broadcasted message. The message contains a table of RSSI values toward all links (other wireless outlets) nearby. During the period of one node polling the other nodes are in the “listening” mode, so there is no interference or superposition of signals between them. The broadcasted message is received by the controller as well as by other nodes which update their RSSI tables with the values of signal strength received for that link. The nodes are able to receive the message from the controller as well as from neighboring nodes. Once the message is received, the RSSI analyzer saves the received values in the local database and waits for the next 100ms, to poll another node inside a room. After a polling cycle, the controller can generate a functional status by monitoring the principal components, extracted from the matrix of RSSI values, as explained in the previous section.

Smart outlets and light switches (shown in Fig. 3), presented in details in [5] and [34], fit into existing electrical installations, power sockets on the wall. Smart outlets provide power to electrical devices with standard flat, two-pole AC power plug (CEE 7/16) which is designed for voltages up to 250V and currents up to 2.5A. Besides simple on/off switching, sockets and light switches are able to pass any percentage of power to the consuming electric device (e.g. light dimmer). IEEE 802.15.4 transceiver (2.4GHz Zigbee) is used as the wireless communication module. Smart outlets are powered from 220-240Vac ( $\pm 10\%$ ) 50Hz current electric power supply. It is an inexpensive and the safest way to provide full compatibility with the regulatory requirements. With an average current of 35mA and the operational voltage of 3.3V for an outlet and 2.4V for a switch, the power supply consumption is approx. 0.12W per an outlet and 0.08W per a switch.



**Fig. 3.** The smart power outlet and smart light switch; the retrofit design that fits into existing electrical installation on the wall (CEE 7/16 standard)

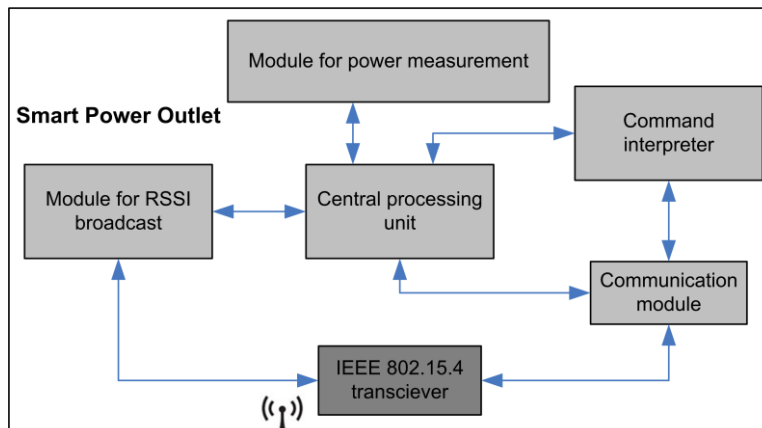


**Fig. 4.** The smart power outlet software design. Smart power outlet is comprised of: module for RSSI broadcast which sends a broadcast message on each polling instruction received from the home controller; the communication module which establishes Zigbee communication protocol with the controller and other smart nodes; the command interpreter which executes the switch and the dimming control; and the module for power measurement which provides consumption data

The smart outlets and light switches incorporate specific firmware which is implemented to enable: (1) the access to the consumption overview on

demand, (2) switching the plugged devices on or off, and (3) environmental sensing by broadcasting RF messages to neighboring nodes. The firmware modules are illustrated in Fig. 4.

The module for power measurement sends its current values periodically (each second) to the home controller. The power consumption for daily, weekly and monthly basis are processed within the home controller and stored into the local database. The module for RSSI broadcast waits for an event from the home controller which actuates the RSSI message broadcasting. The same module receives broadcasted messages from other nodes during the polling cycle. Parsed message is saved in the structure, which is provided to the home controller after the node is polled. Command interpreter executes commands received from the home controller, such as dimming control, switching the plugged device on or off, etc. The smart light switch firmware design is similar to the smart outlet firmware.

## 5. Experimental Results for Human Presence Detection

The test bed described in the previous section was installed in two buildings. In the first building, walls were made of concrete parts (exterior wall) and gypsum attached to the steel construction (interior wall) isolated with fiberglass wool. The gypsum wall thickness was 15cm and the concrete wall was 30cm. In the second building, the walls were made of aluminum and plastic covers, 30cm thick and mounted on steel construction, isolated with fiberglass wool. In each building a room was selected and four smart nodes were installed and placed strategically. Three of them (smart outlets) have been positioned at an elevation of 40cm above the floor and the last one (smart switch) was positioned at an elevation of 120cm above the floor. The testing room made of concrete and gypsum walls (further referred to as *R1*) was 536×530cm, whereas the room with aluminum and plastic walls (further referred to as *R2*) was 960×580cm large. The rooms' layouts and the positions of a subject (shown as points *P1-P5* for *R1*, apropos *P1-P6* for *R2*) and nodes positions (shown as squares *N1-N4*) are illustrated in Fig.5.

Coordinates of each node in *R1*, relatively to the central position, as well as positions of a testing subject, are given in Table 1. All the coordinates are given in cm, and measured relatively to the central position. The central position is located in the down left corner.

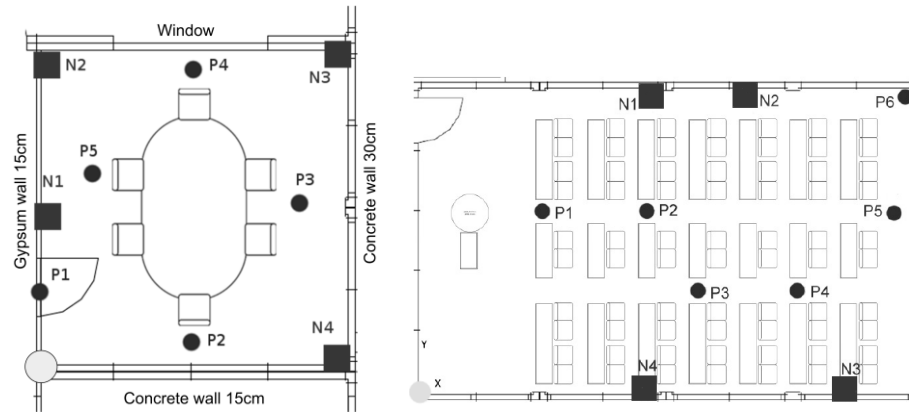


**Fig. 5.** The experimental rooms' layout. On the left - the room with concrete and gypsum walls; on the right - the room with aluminum walls with plastic slices

**Table 1.** Human subject's and wireless nodes' positions in R1

Node name	Node coordinates	Subject's position	Subject's coordinates
N1	(73, 211)	P1	(0, 78)
N2	(54, 477)	P2	(270, 75)
N3	(474, 428)	P3	(424, 254)
N4	(519, 66)	P4	(306, 420)
-	-	P5	(120, 255)

Coordinates of each node in *R2*, relatively to the central position, as well as positions of a testing subject are given in Table 2. The central position is also located in the down left corner. The coordinates are given in cm.

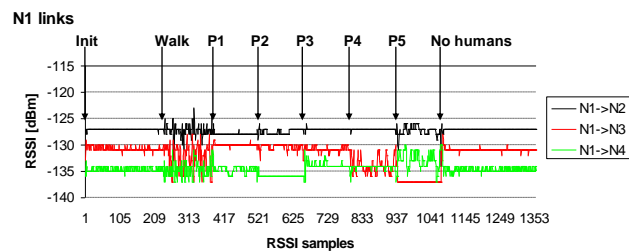
**Table 2.** Human subject's and wireless nodes' positions in R2

Node name	Node coordinates	Subject's position	Subject's coordinates
N1	(410,530)	P1	(220,305)
N2	(600,530)	P2	(410,305)
N3	(795,40)	P3	(500,150)
N4	(410,40)	P4	(690,150)
-	-	P5	(945,305)
-	-	P6	(955, 500)

According to scattering, diffraction, absorption and reflection of the signal in these environments, two test scenarios were defined. In the first scenario, the room was empty for a period of two minutes, and no detection was reported. Once a subject entered the room, he performed clockwise walking

around the table within the room, by passing the positions  $P1-P5$ , from the Fig. 5 - left. After one minute of walking, the subject was standing in each position  $P1-P5$ , for a minute, without movements. The scenario tried to confirm the hypothesis that the detection of human presence or movement is possible by analyzing the extracted principal components from the sets of RSSI variations retrieved from each wireless link. Sets of raw RSSI samples, before PCA processing, are logged and presented in Fig. 6. The values are given in dBm, but the idea is that the algorithm takes raw 8bit values into the processing. In that case no additional conversions are necessary during the runtime. The 8bit RSSI value is in signed 2's complement on a logarithmic scale with 1-dB step and must be corrected with an RSSI offset to get the real RSSI value in dBm. For CC2530 transceiver, the RSSI offset is 73 dB. Real RSSI is calculated by subtracting the RSSI offset from the converted 8bit RSSI value.

From the Fig. 6 it can be noticed that in the position  $P1$  the RSSI variation was emphasized only at the link  $N1 \rightarrow N4$  in both directions. It is explained as a result of signal reflection by the human body which was very close to the line-of-sight between outlets  $N1$  and  $N4$ . In the position  $P2$ , the human body shadowed the links  $N1 \rightarrow N4$  and  $N4 \rightarrow N1$ , and the most of the radio signal was absorbed by the human body which is the main reason for lower RSSI values. In the position  $P2$ , the links  $N2 \rightarrow N4$  and  $N4 \rightarrow N2$  were distorted with the reflection by the human body. Therefore, high RSSI variation in the position  $P2$  for links between outlets  $N2$  and  $N4$  can be noticed. Moreover, the position  $P2$  had slight influence to the links  $N1 \rightarrow N3$  and  $N3 \rightarrow N1$  that were distorted by the vicinity of human body which slightly reflected the signal. The human position  $P3$  mostly absorbed the signal from the links  $N2 \rightarrow N4$  and  $N4 \rightarrow N2$ , and reflected the signals from the links  $N3 \rightarrow N4$ ,  $N4 \rightarrow N3$  and  $N1 \rightarrow N4$ ,  $N4 \rightarrow N1$ . Position  $P4$  shadowed the links  $N1 \rightarrow N3$  and  $N3 \rightarrow N1$  and absorbed the signal. The position  $P5$  shadowed the links  $N1 \rightarrow N3$  and  $N3 \rightarrow N1$  and reflected the signals from the rest of links, except for  $N3 \rightarrow N4$  and  $N4 \rightarrow N3$  which were far from the current human position. At the end of the experiment the room was empty again for two minutes.



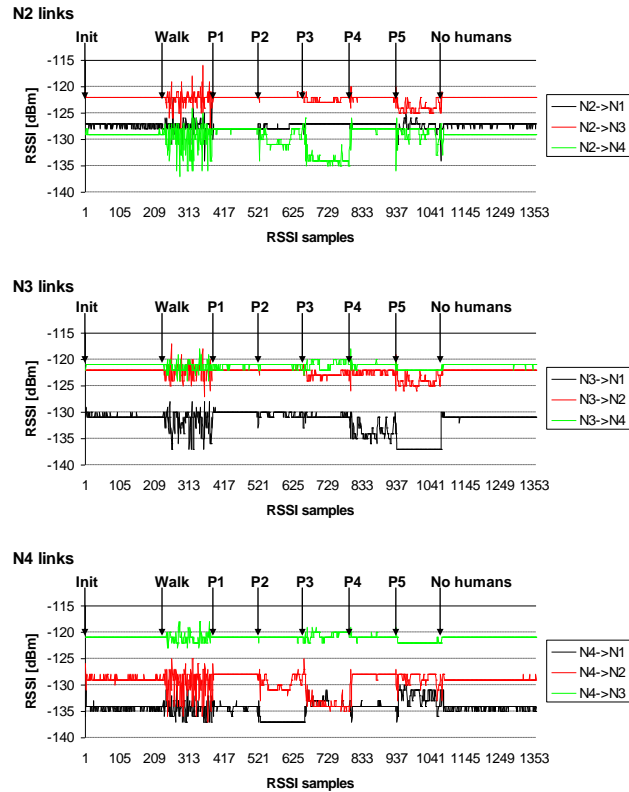


**Fig. 6.** Raw RSSI samples data observed in the first experimental room – R1

From the aspects of radio irregularity feature, the conclusion for the first scenario can be deduced: (1) RSSI for all wireless nodes that have communicated far from the human, varied slightly or had a constant value. (2) When the human was positioned closer to a node, without obstructing the line-of-sight, RSSI varied significantly. The larger variation is explained as the consequence of the signal reflection. (3) When the human obstructed the line-of-sight on one link, the RSSI did not vary much comparing to the other links, but was diverse comparing to the initial values.

It can be clearly noticed that the appearance of a human subject induced RSSI variations in the environment. Particularly, during subject's walking, RSSI variations have been emphasized at all links.

Once the data set is collected for a number of samples (interval  $p$  – the testing was performed for the interval of 12, 24 and 36 RSSI samples) the matrix  $Nod$  given by (2) is formed, for each link. After the matrix  $X$  is created and the matrix  $C_x$  is calculated, the principal components are extracted. The graphical presentations of principal components stored in the *Feature Vector*  $fv$  for the time interval of 550 seconds are shown in Fig. 7, Fig. 8 and Fig. 9,

depending of the interval  $p$  (12, 24 and 36, respectively). Different values for  $p$  are used to experimentally determine the optimal number of samples that can achieve accurate detection and preserve fast system response. The first 200 principal components are used to define the detection bound, and this phase is known as the training phase. During the training phase no human should be present in the room, otherwise high detection bound can be set. The detection bound is calculated as the maximal value of principal components from the training phase. The values higher than the calculated bound report detection.

In the Fig. 7 the result of the applied PCA for the shifting interval  $p$  which includes 12 samples is shown. The first high peak (after the sample 200) reports the presence of a human. As defined in the scenario, the human was walking for a minute (the following 200 samples). During the motion, the principal components powers are strongly emphasized and human presence can be easily detected with 100% accuracy. The human standing without movements is less expressed on principal components and the detection accuracy is lower. The following high peaks show the transitions from each position  $P1$ - $P5$  to the next one. The defined human positions gradually affect the radio links in the room. All the links are not immediately obstructed with the human body and high discrepancies between them exist. Some of the links would still have low RSSI variations before their line-of-sight becomes intersected. As the human moves to the centre of the room (positions  $P3$ ,  $P4$  and  $P5$ ), the power of principal components increases. The overall detection accuracy, with  $p$  defined to include 12 samples, is approx. 75.3% for human presence (which includes walking and standing in each position  $P1$ - $P5$ ), whereas the accuracy for the empty room detection is 100%.

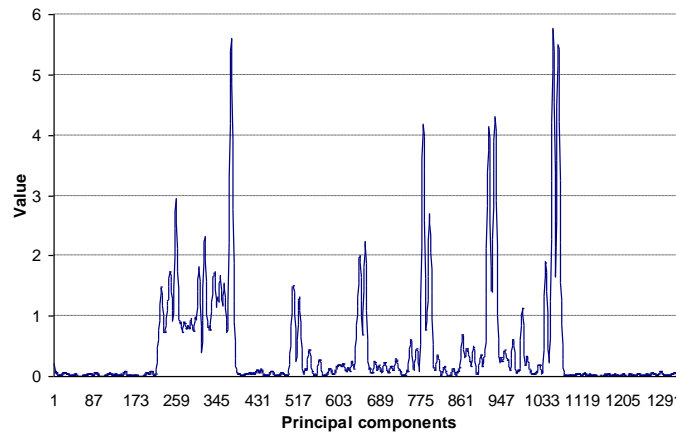


**Fig. 7.** PCA analysis results for R1 - an array of principal components for the shift interval defined to be  $p=12$  and the input data representing the matrix  $X$  which contains standard deviations of the RSSI samples

Around the sample 400 the subject moved to the position *P1* and stopped. Although the principal components in that position have low power, the most of them exceed the detection bound. The power of principal components is lower in the *P1*, because only several links are affected with the human body.

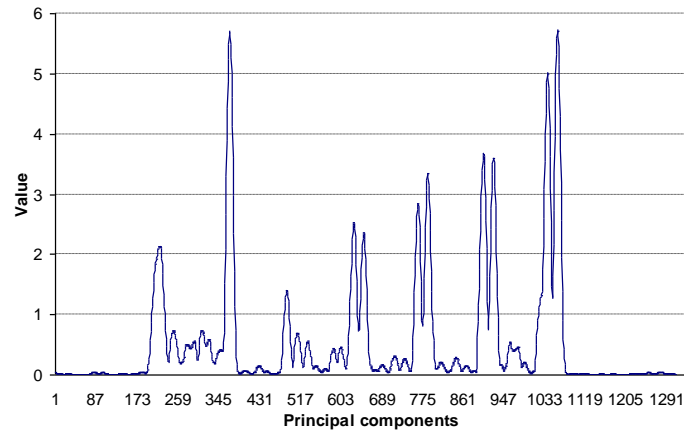


**Fig. 8.** PCA analysis results for R1 - an array of principal components for the shift interval defined to be  $p=24$  and the input data representing the matrix  $X$  which contains standard deviations of the RSSI samples

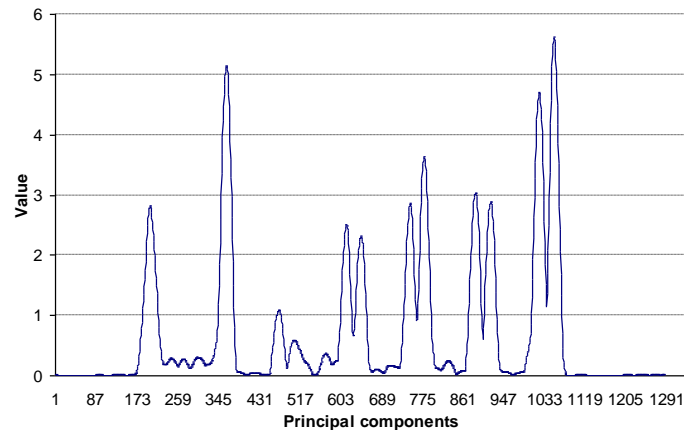


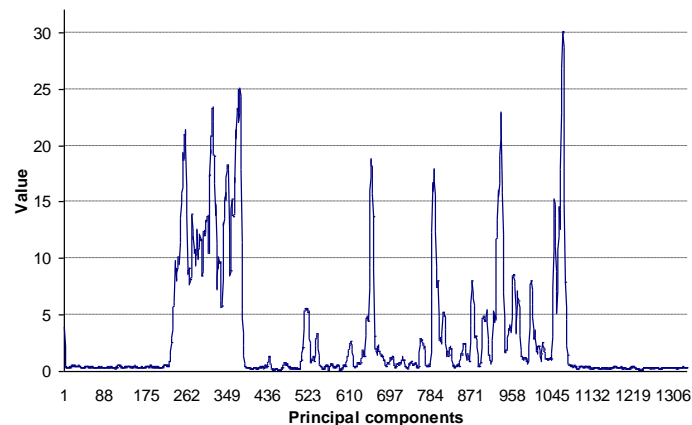
**Fig. 9.** PCA analysis results for R1 - an array of principal components for the shift interval defined to be  $p=36$  and the input data representing the matrix  $X$  which contains standard deviations of the RSSI samples

In the Fig. 8, the shifting interval is comprised of 24 samples. The detection accuracy is approx. 93.6% for human presence. The empty room detection is 100% accurate. This shifting interval is more robust to false detections. In Fig. 9, the shifting interval is comprised of 32 samples, which is

the most robust to errors and the human presence detection is 97.8% accurate, whereas empty room is detected in 100% cases.

The false detection rate decreases as the number of samples of the interval  $p$  grows, but the processing time is increasing for the calculation of principal components. For  $p$  is 24 and 36, the polling time of 100ms for each outlet is insufficient, because the algorithm can not extract the eigenvalues in 400ms, which is the time period until the next polling cycle. From the number of experiments, the optimal polling time per outlet is determined to be 200ms if  $p$  is 24, and 350ms if  $p$  is 36. For  $p$  is 12, the polling time of 100ms is satisfactory but the false detections rate is higher. Therefore, the solution for improving the processing speed is to implement an incremental algorithm which calculates eigenvalues only by using the previously calculated principal component as a predictor. The predictor is combined with the RSSI samples stored in  $n \times 1$  vector, where  $n$  is the number of links. Instead of processing  $p \times p$  matrix of RSSI samples, the improved algorithm calculates principal components from the vector. The fuzzy reasoning filter [35] would be useful to additionally isolate all the values below the calculated bound and the results would become more accurate. The detailed description of the filter and the incremental algorithm are not considered in this paper.

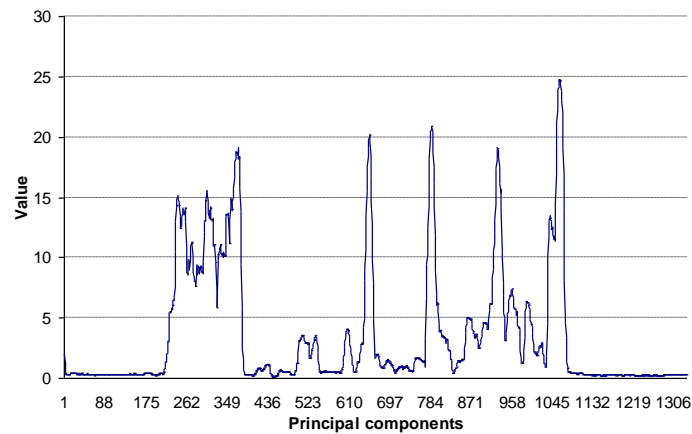
Another approach is the definition of the matrix  $X$  from (4), as the matrix of raw RSSI samples, instead of standard deviations. In that case, the matrix  $X$  is equal to the matrix  $Nod$  from (2) and the definition of the matrix does not require the calculation of the standard deviation per interval  $p$ . In the Fig. 10 the result of the applied PCA algorithm for the interval  $p$  which includes 12 raw samples is shown. Human presence detection accuracy is 76.4% and the detection of the empty room is accurate in 99.6% cases.



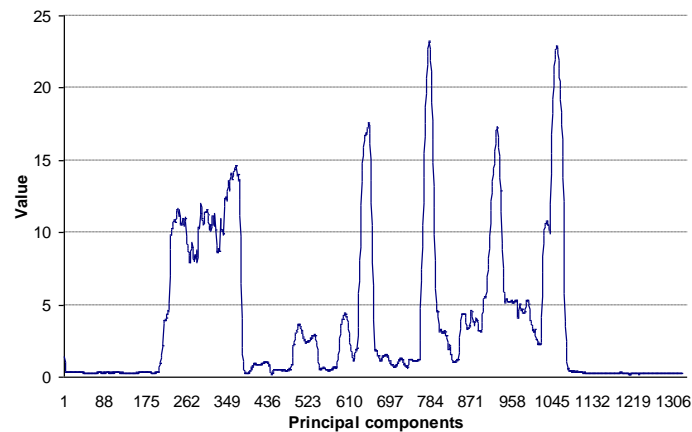
**Fig. 10.** PCA analysis results for R1 - an array of principal components for the shift interval defined to be  $p=12$  and the input data representing the matrix  $X$  which contains raw RSSI samples

In the Fig. 11 and Fig. 12 the extracted principal components for raw RSSI inputs and  $p$  defined to be 24 and 36 are shown, respectively. The false

detection rate decreases as the interval  $p$  grows. For  $p=24$ , human detection accuracy is 94.2% and the empty room detection accuracy is 100%, whereas for  $p=36$ , human detection accuracy is 97.9%, and the empty room detection accuracy is 100%. Unfortunately, the same issue with the increased latency of the system response exists. However, the detection accuracy increases when raw values are used instead of standard deviations. The detection accuracy of these two types of inputs for the variation of the  $p$  interval is shown in Fig. 13.

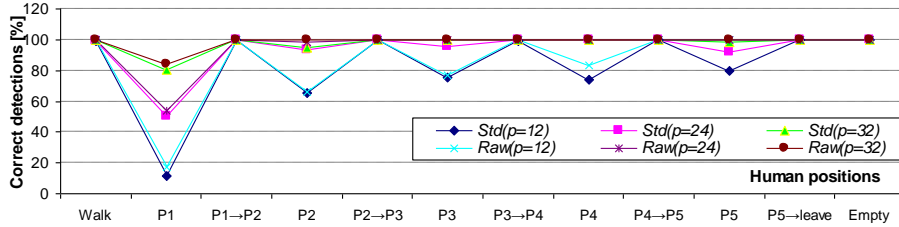


**Fig. 11.** PCA analysis results for R1 - an array of principal components for the shift interval defined to be  $p=24$  and the input data representing the matrix  $X$  which contains raw RSSI samples



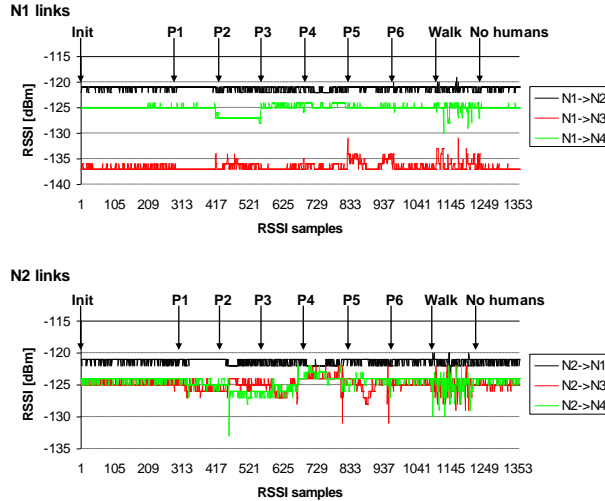
**Fig. 12.** PCA analysis results for R1 - an array of principal components for the shift interval defined to be  $p=36$  and the input data representing the matrix  $X$  which contains raw RSSI samples

## System Design for Passive Human Detection using Principal Components of the Signal Strength Space



**Fig. 13.** The detection accuracy is shown for both standard deviations and raw values, including  $p=12$ , 24 and 36. The accuracy is given for human presence detection during: walking, standing in positions  $P1$ - $P5$ , and transition from  $Pn$  to  $Pn+1$  (where  $n$  counts from 1 to 5). The detection of the empty room is shown as well

The test scenario in R2 was slightly different from the previous one. The room R2 was empty for a period of two minutes, and no detection was reported. Once a human stepped into the room, he was standing in each position  $P1$ - $P6$  from the Fig. 5-right for one minute without movements. After samples from all positions were collected, the subject performed one minute of walking within the room by passing the positions  $P1$ - $P6$ . Because of the walls' structure, this environment formed a Faraday's cage. The signal was interfered with the reflection by the walls and the RSSI variation is noticed even in the empty room. Sets of raw RSSI samples retrieved from each link between nodes, before PCA processing are logged and presented in Fig. 14.



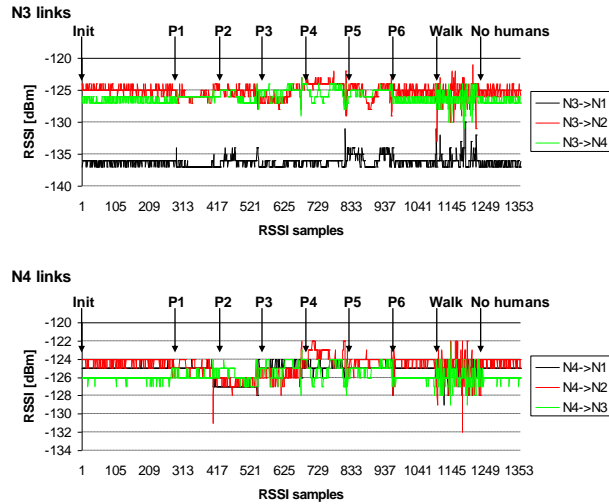


**Fig. 14.** Raw RSSI samples data observed in the second experimental room – R2

In the position  $P1$ , small RSSI variations were present on several links. In the position  $P2$ , the human body shadowed the links between nodes  $N1$  and  $N4$ , so the most of the signal strength was absorbed. The position  $P2$  had slight influence to the links  $N1 \rightarrow N3$ ,  $N3 \rightarrow N1$ ,  $N2 \rightarrow N4$  and  $N4 \rightarrow N2$  that were distorted by the vicinity of human body which induced the signal reflection. The human position  $P3$  was responsible for signal reflection between nodes  $N2$  and  $N4$  and also for the links  $N2 \rightarrow N3$  and  $N3 \rightarrow N4$  in both directions. The position  $P4$  caused very strong signal reflection for links between nodes  $N2$  and  $N4$ , and also  $N3$  and  $N4$ , whereas the signals between nodes  $N2$  and  $N3$  were absorbed. The human body position  $P5$  induced RSSI variations on links between nodes  $N1$  and  $N3$ . The strongest impact on the signal strength in the position  $P5$  was noticed for the links between nodes  $N2$  and  $N3$ . The influence of the position  $P5$  in combination with the wall reflection was responsible for the increased RSSI variation. The position  $P6$ , which was the furthest position from all nodes, did not affect the RSSI. Therefore, human presence detection was not possible. The position  $P6$  is defined as the “blind position”, which is out of the detection scope. At the end of the experiment the human was walking around the room, by moving closer to nodes  $N2$ ,  $N3$  and  $N4$ , and radio links therein, without obstructing the line-of-sight between nodes  $N1$  and  $N2$ . After one minute of walking, the room was empty, as it was at the beginning of the experiment, for a minute.

After the matrix  $X$  is created by using (4) and the covariance matrix  $C_X$  (7) is calculated by using standard deviations of the RSSI samples for specific interval  $p$ , the principal components are extracted and stored into the *Feature Vector*  $fv$ . The graphical presentations of the principal components

System Design for Passive Human Detection using Principal Components of the Signal Strength Space

for 1420 samples (568 seconds) with different values of the interval  $p$ , are shown in Fig. 15, Fig. 16 and Fig. 17.

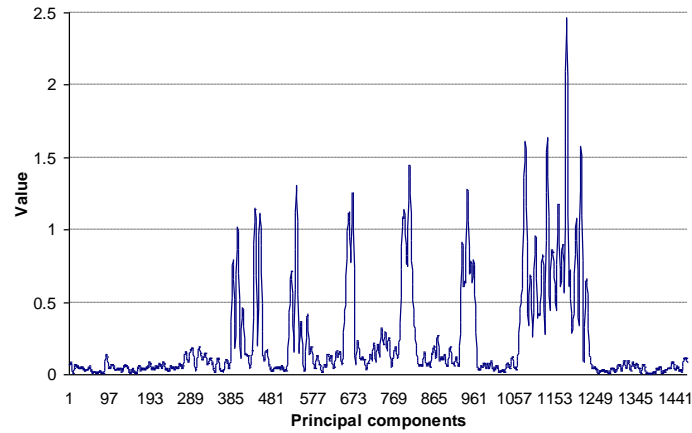


**Fig. 15.** PCA analysis results for R2 - an array of principal components for the shift interval defined to be  $p=12$  and the input data representing the matrix  $X$  which contains standard deviations of the RSSI samples

For principal components around the samples 500 and 1000, from the Fig. 15, a higher probability of false detections occurs. The detection bound is also calculated during the initial 200 samples when the room was empty. The detection accuracy using PCA in R2 with  $p$  defined to include 12 samples is around 53.9% for presence, and 100% for the empty room detection.

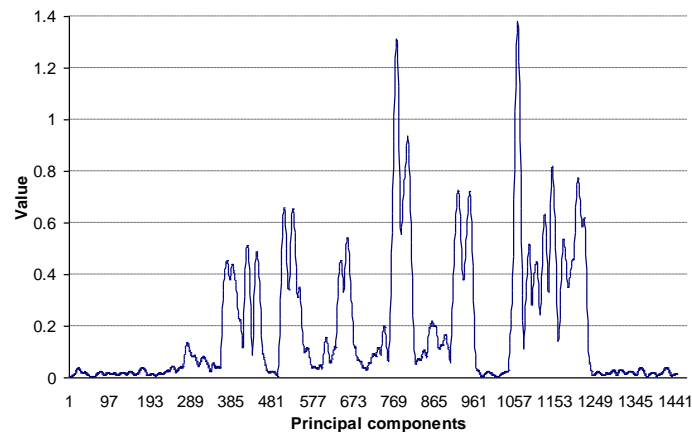


**Fig. 16.** PCA analysis results for R2 - an array of principal components for the shift interval defined to be  $p=24$  and the input data representing the matrix  $X$  which contains standard deviations of the RSSI samples

In the Fig. 16 and Fig. 17, the shifting interval is comprised of 24 and 36 samples, respectively. For the case when  $p$  is 24 samples the detection

accuracy is around 81.6% for presence and 100% for the empty room. For the case when  $p$  is 36 samples the detection accuracy is around 90.4% for presence and 100% for the empty room.

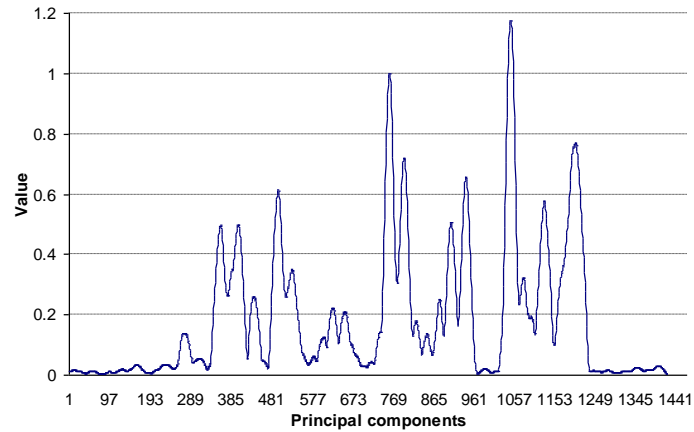


**Fig. 17.** PCA analysis results for R2 - an array of principal components for the shift interval defined to be  $p=36$  and the input data representing the matrix  $X$  which contains standard deviations of the RSSI samples

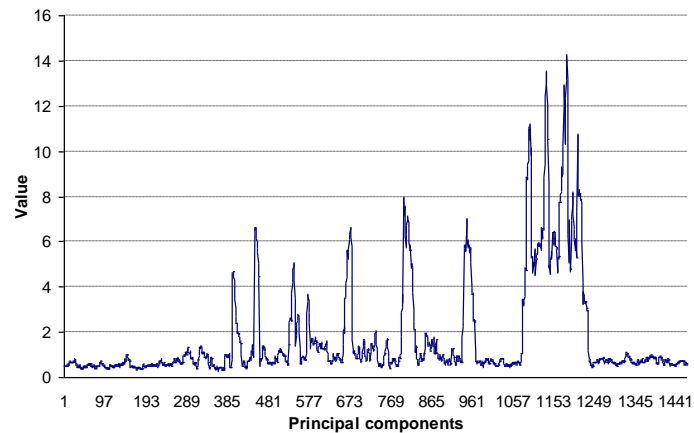


**Fig. 18.** PCA analysis results for R2 - an array of principal components for the shift interval defined to be  $p=12$  and the input data representing the matrix  $X$  which contains raw RSSI samples

The wall reflection which was interfered with the reflection by the human body mostly affected signals in this environment. Although the initial radio map was disturbed in this environment, human presence and motion were successfully recognized for most of the positions. Only for the “blind position”

System Design for Passive Human Detection using Principal Components of the Signal Strength Space

$P_6$ , the detection accuracy was very low. The integration of the additional outlets would improve the radio coverage in large rooms.

Another approach is the definition of the matrix  $X$  (4) as the matrix of raw samples, as in the previous experiment. In Fig. 18 the result of the applied PCA algorithm for the shifting interval  $p$  which includes 12 raw samples is shown. The human presence detection accuracy is 54.1% and the accuracy of the empty room detection is 99.1%. In Fig. 19 and Fig. 20, the result of the applied PCA for the interval  $p$  which includes 24 and 36 raw samples is shown, respectively. The false detection rate decreases as the number of  $p$  samples grows, but larger  $p$  implicates longer latency which should be optimized with an iterative method combined with the fuzzy filter.

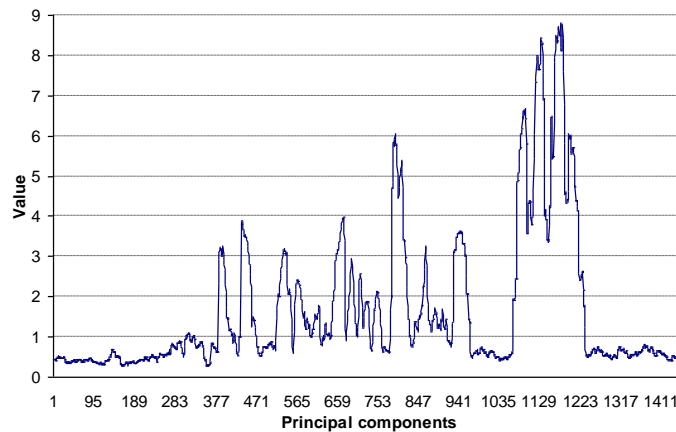


**Fig. 19.** PCA analysis results for R2 - an array of principal components for the shift interval defined to be  $p=24$  and the input data representing the matrix  $X$  which contains raw RSSI samples

The human presence detection accuracy for the  $p$  interval of 24 samples is approx. 83%, whereas the accuracy for the empty room detection is 100%. The human presence detection accuracy for  $p=36$  samples is 91.5%, whereas the empty room detection accuracy is 100%. The detailed error distribution, depending of  $p$  and the input samples, is shown in Fig. 21.

As concluded for the previous experiment, the same conclusion can be deduced for this experiment: the detection accuracy increases when using raw RSSI values, in contrary to standard deviations of the RSSI.

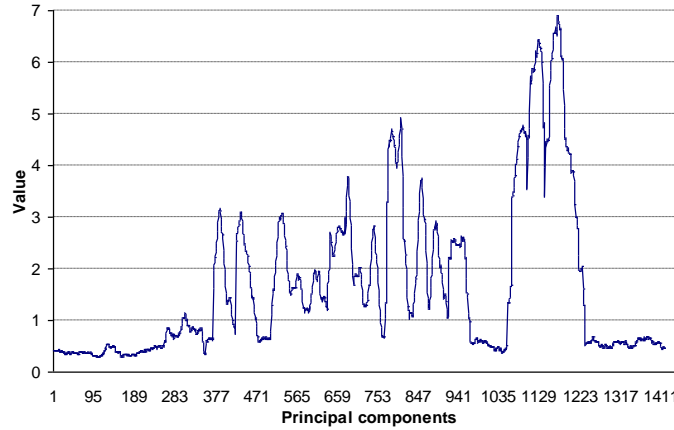


**Fig. 20.** PCA analysis results for R2 - an array of principal components for the shift interval defined to be  $p=36$  and the input data representing the matrix  $X$  which contains raw RSSI samples

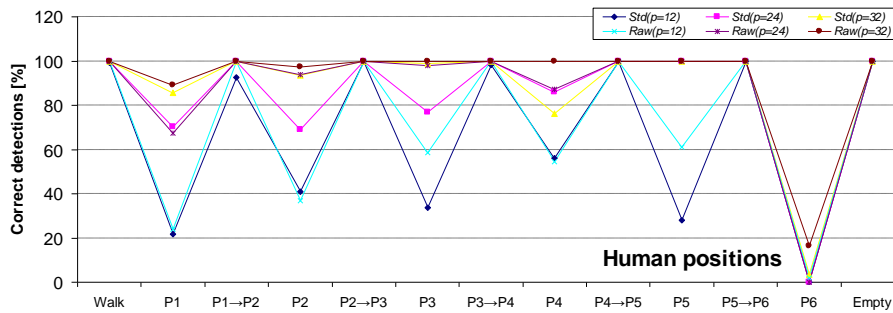


**Fig. 21.** The detection accuracy is shown for both standard deviations and raw values, including  $p=12$ , 24 and 36. The accuracy is given for human presence detection during: walking, standing in positions  $P1$ - $P6$ , and moving from  $Pn$  to  $Pn+1$  (where  $n$  is 1 to 6). The detection of the empty room is also shown

### 5.1. Energy Saving Experiment

The integration of the provided energy-saving system [5] with the proposed method for human presence detection, enabled a prototype realization. The prototype has been installed in four, the least frequently occupied rooms in an average household. The primary goal was to demonstrate the proposed method operating in real conditions for the energy saving. Energy saving has been achieved by utilizing two approaches: (1) if there is nobody present in the room for more than 10 seconds, turn the light in that room off, (2) always

decrease the brightness of lights in the household by 10%, what should be unnoticeable to users but saves an amount of energy. To be able to provide the comparison between the regular human behavior on energy saving and the proposed prototype, 8 bulbs of 100W combined with 12 smart outlets and 4 smart light switches have been installed in each room (4 smart nodes and 2 bulbs per a room). In each room, one bulb was under regular control (manual on/off switching), which included the worst case - a user leaves the light on after leaving a room. The second bulb was under automatic control. The automatic control is achieved by using predefined power behavior schemes, which define system responses on human presence detection events. Operational “energy saving” mode switched off the light after 10 seconds when no-presence was reported by the RSSI analyzer module (from Fig. 2), and also switched the light on, almost immediately, when a human entered the room. In each room, both bulbs (lamps) were plugged to smart outlets in order to provide the power consumption logging for the detailed comparison.

The experiment has been performed during one working day with four-member family (two adults and two kids). Two bedrooms, one bathroom and a foyer have been defined as test rooms, where the real presence of humans was the most dynamic. The test subjects performed the normal behavior at home, trying to manually switch off the lights in each unoccupied room. All the rooms were properly covered with the radio signal and no “blind positions” were recognized. The walls were made of concrete and brick blocks, 30cm thick for exterior walls and 20cm for interior wall.

Supported with the proposed presence detection algorithm, the energy consumption used for lights was decreased from 1220 W/h to 730 W/h at the end of the day. In the Fig. 22, the power consumption, achieved by using regular and automatic control is shown, per each hour during the experiment.

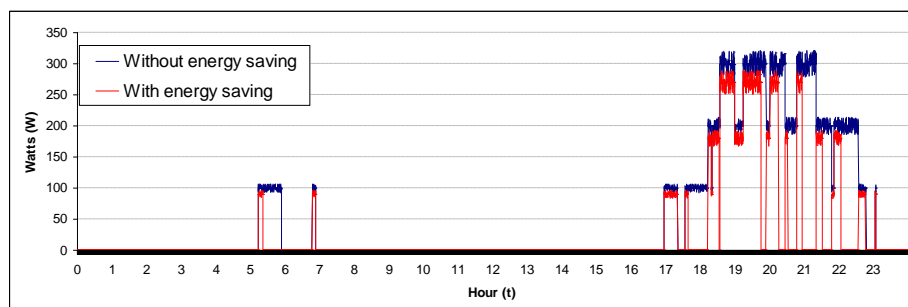


**Fig. 22.** Measured power consumption in the experimental house by comparing manual interaction for lights control (blue) and automatic “energy saving mode” (red)

For this experiment, PCA used inputs of  $p=24$  raw samples. With the polling time of 200ms per an outlet, the detection could be reported on each 800ms, including additional 600ms for the PCA processing and the generation of a functional status. This is the optimal time with the high accuracy, suitable for this experiment. For  $p=36$  samples, the functional

status can be generated after approx. 2.8s (including the polling cycle for detection), which is too long. The polling time of 200ms is acceptable when the number of smart nodes is four or less. For additional smart nodes, the polling time has to be reduced to 100ms. The detection accuracy for  $p=12$  (100ms polling) is not optimal.

## 6. Conclusion

PCA presents a simple method for extracting relevant information from confusing and large data sets. It is a variable reduction procedure and is useful when samples are obtained on a large number of variables that are mutually correlated. PCA helps identifying patterns in the data, and expressing the data in a way that highlights their similarities or differences. Because of this variables redundancy, it is possible to reduce a large set of observed variables into a smaller number of principal components, while retaining as much as possible of the variation present in the original data set.

The presented article confirms the hypothesis that human presence detection is possible by applying the PCA to the set of RSSI samples obtained from radio links between wireless power outlets. The experimental results show that PCA inputs, given in a form of raw RSSI samples, provide more accurate results for human presence detection, than the inputs which describe the dispersion of the signal, such as standard deviation. More accurate detection requires larger set of input samples, which implicates larger processing time and overall system response delay. For the future improvement, the testing would be performed in another buildings made of different materials, with dynamic changes of the furniture layout which can introduce additional interferences (noise) to the system. The testing in such environments would be helpful for finding patterns that would enable the definition of a fuzzy reasoning algorithm which would improve the accuracy of human presence detection. Additionally, an incremental method needs to be defined which would speed up the processing time, and the overall system's response for the larger number of additional wireless smart nodes.

The presented solution can significantly conserve electric energy in a household, by executing automatic operations which switch off power on devices that are not used for a specified period of time. The test subjects confirmed that 1s to 1.5s are acceptable for the functional status generation. However, the further intention is to decrease the system's response without decreasing the accuracy of the proposed algorithm.

**Acknowledgement.** This work was partially supported by the Ministry of Education and Science of the Republic of Serbia under Grant TR-32029 and by the Secretary of Science and Technology Development of the Province of Vojvodina under Grant 114-451-2434/2011-03.

## References

1. Jahn, M., Jentsch, M., Prause, C.R., Pramudianto, F., Al-Akkad, A. and Reiners, R.: The energy aware smart home. In Proceeding of the 5th International Conference on Future Inform. Technologies (FutureTech '10), Korea, 1-8. (2010)
2. Sundramoorthy, V., Liu, Q., Cooper, G., Linge, N. and Cooper, J.: DEHEMS: a user-driven domestic energy monitoring system. In Proceedings of Internet of Things (IOT '10), 1-8. (2010)
3. Song, G., Ding, F., Zhang, W. and Song, A.: A wireless power outlet system for smart homes. *IEEE Transactions on Consumer Electronics*, Vol. 54, No. 4, 1688-1691. (2008)
4. Han, J., Lee, H. and Park, K.R.: Remote-controllable and energy-saving room architecture based on ZigBee communication. *IEEE Transactions on Consumer Electronics*, Vol. 55, No. 1, 264-268. (2009)
5. Mrazovac, B., Bjelica, M.Z., Papp, I. and Teslic, N.: Towards ubiquitous smart outlets for safety and energetic efficiency of home electric appliances. In Proceedings of International Conference on Consumer Electronics (ICCE '11), Berlin, Germany, 324-328. (2011)
6. European Regulators' Group for Electricity and Gas, Smart Metering with a Focus on Electricity Regulation, Document E07- RMF-04-03. (2007)
7. Ababneh, N.: Radio irregularity problem in wireless sensor networks: New experimental results. In Proceedings of IEEE Sarnoff Symposium, Princeton, USA, 1-5. (2009)
8. Zhou, G., He, T., Krishnamurthy, S., and Stankovic, J.A.: Impact of radio irregularity on wireless sensor networks. In Proceedings of the 2nd International Conference on Mobile Systems, Applications and Services (MobiSys '04), 125-138. (2004)
9. Youssef, M., Mah, M., and Agrawala, A.: Challenges: device-free passive localization for wireless environments. In Proceedings of the 13th annual ACM International Conf. on Mobile Computing and Networking, pp. 222–229 (2007)
10. Woyach, K., Puccinelli, D. and Haenggi, M.: Sensorless sensing in wireless networks: Implementation and measurements. In Proc. of 2nd Intl. Workshop on Wireless Network Measurement (WinMee'06), Boston, USA, 1-8. (2006)
11. Puccinelli, D., Foerster, A., Puiatti, A. and Giordano, S.: Radio-Based Trail Usage Monitoring with Low-End Motes. In Proceedings of the 7th IEEE International Workshop on Sensor Networks and Systems for Pervasive Computing (PerSens '11), Seattle, USA, 196-201. (2011)
12. Lee, P.W.Q., Seah, W.K.G., Tan, H.P. and Yao, Z.X.: Wireless Sensing without Sensors - An experimental study of motion/intrusion detection using RF irregularity. *Journal of Measurement Science and Technology*, Special Issue on Wireless Sensor Networks: Designing for real-world deployment and deployment experiences, Vol. 21, No. 12, (2010)
13. Lin, W.C., Seah, W.K.G. and Li, W.: Exploiting radio irregularity in the internet of things for automated people counting. In Proc. of the 22nd IEEE Symposium on Personal, Indoor, Mobile and Radio Comm. (PIMRC '11), Toronto Canada, (2011)
14. Hussain, S., Peters, R. and Silver, D.L.: Using received signal strength variation for surveillance in residential areas. In Proc. of the 9th ACM/IEEE Intl. Conf. on Information Processing in Sensor Networks (IPSN '10), Vol. 6973, 1-6. (2008)
15. Kaltiokallio, O., Bocca, M. and Eriksson, L.: Distributed RSSI processing for intrusion detection in indoor environments. In Proc. of 9th ACM/IEEE

- International Conf. on Information Processing in Sensor Networks (IPSN '10), 404-405. (2010)
16. Puzo, E.L., Brenner, R.P., Walker, T.O. and Anderson, C.R.: The Matrix: a roadside wireless security system. In Proceedings of Virginia Tech Symposium on Wireless Personal Communications, Virginia, USA, (2011)
  17. Patwari, N. and Wilson, J.: RF sensor networks for device-free localization and tracking. In Proceedings of the IEEE, Vol. 98, No. 11, 1961-1973. (2010)
  18. Deak, G., Curran, K. and Condell, J.: History Aware Device-free Passive (DfP) Localisation. Image Processing & Communications Journal, vol. 16, no. 3-4, pp. 21-30. (2011)
  19. Zhang, D., Ma, J., Chen, Q. and Ni, L. M.: An RF-Based System for Tracking Transceiver-Free Objects. In Proceedings of the Fifth Annual IEEE International Conference on Pervasive Computing and Communications, (PerCom '07), pp. 135-144. (2007)
  20. Zhang, D. and Ni, L. M.: Dynamic Clustering for Tracking Multiple Transceiver-Free Objects. In Proceedings of the Seventh Annual IEEE International Conf. on Pervasive Computing and Communications (PerCom '09), pp. 1-8. (2009)
  21. Moussa, M. and Youssef, M.: Smart Devices for Smart Environments: Device-free Passive Detection in Real Environments. In Proceedings of the Seventh Annual IEEE International Conference on Pervasive Computing and Communications (PerCom '09), pp.1-6. (2009)
  22. Shah, N., Tsai, C.-F. and Chao, K.-M.: Monitoring appliances sensor data in home environment: Issues and challenges. In Proceedings of IEEE Conference on Commerce and Enterprise Computing (CEC '09), 439-444. (2009)
  23. Chen, C.-S. and Lee, D.-S.: Energy saving effects of wireless sensor networks: A case study of convenience stores in Taiwan, Sensors '11, Vol.11, No.2, 2013-2034. (2011)
  24. Chao, K.-M., Shah, N., Matei, A., Zlamaniec, T., Li, W, Lo, C.-C. and Li, Y.: Intelligent interactive system for collaborative green computing. In Proceedings of CSCWD '11, 690-697. (2011)
  25. Pensas, H., Raula, H. and Vanhala, J.: Energy efficient sensor network with service discovery for smart home environments. In Proc. of SENSORCOMM '09, 399-404. (2009)
  26. Zhou, Z., Xiang, X. and Wang, X.: An energy-efficient data-dissemination protocol in wireless sensor networks. In Proc. of International Symposium on a World of Wireless, Mobile and Multimedia Networks (WoWMoM'06), 13-22. (2006)
  27. Mrazovac, B., Bjelica, M.Z., Todorovic, B.M., Miljkovic, A. and Samardzija, D.: Using Radio Irregularity for Increasing Residential Energy Awareness. Telfor Journal, vol. 4, no. 1, pp. 31-36. (2012)
  28. Mrazovac, B., Bjelica, M.Z., Kukolj, D., Todorovic, B.M. and Samardzija, D.: A Human Detection Method for Residential Smart Energy Systems Based on Zigbee RSSI Changes. IEEE Transactions on Consumer Electronics, vol.58, no.3, pp. 819-824. (2012)
  29. Smith, L.I.: A tutorial on Principal Components Analysis. (2002). [Online]. Available: [http://www.sccg.sk/~haladova/principal\\_components.pdf](http://www.sccg.sk/~haladova/principal_components.pdf) (May 2012)
  30. Shlens, J.: A tutorial on Principal Component Analysis: Derivation, Discussion and Singular Value Decomposition. (2003). Available: [http://www.cs.princeton.edu/picasso/mats/PCA-Tutorial-Intuition\\_jp.pdf](http://www.cs.princeton.edu/picasso/mats/PCA-Tutorial-Intuition_jp.pdf) (May 2012)

31. Castells, F., Lasasosa, P.L., Sörnmo, L., Bollmann, A. and Millet-Roig, J.: Principal Component Analysis in ECG Signal Processing. EURASIP Journal on Advances in Signal Processing. Vol. 2007, Article ID 74580. (2007)
32. Jain, A., Duin, R. and Mao, J.: Statistical Pattern Recognition: A Review. IEEE Trans. on Pattern Analysis and Machine Intelligence. Vol. 22, No. 1, 4-37. (2000)
33. Bjelica, M.Z., Mrazovac, B. and Teslic, N.: Evaluation of the Available Scripting Languages for Home Automation Networks: Real World Case Study. In Proc. of TELSIS'11, Nis, Serbia, 611-614. (2011)
34. Mrazovac, B., Bjelica, M.Z., Teslic, N., Papp, I., Temerinac, M.: Consumer-oriented Smart Grid for Energy Efficiency. In Proc. of VDE Kongress 2012, Stuttgart, Germany (2012)
35. Sánchez-Torrubia, M.G. and Torres-Blanc C.: GRAPHS: A Mamdani-type Fuzzy Inference System to Automatically Assess Dijkstra's Algorithm Simulation. International Journal on Information Theory and Applications, Vol. 17, No. 1, 35-48. (2010)

**Bojan Mrazovac** has received BSc and MSc degrees from the Faculty of Technical Sciences, University of Novi Sad, Serbia. He is currently employed as a software design engineer at RT-RK LLC, and he is also working towards his PhD degree at the department for Computer Engineering and Computer Communications, at Faculty of Technical Sciences, Novi Sad. He is currently enrolled in several research projects including home automation and energy aware systems. His expertise also covers the range of embedded platforms and software with the emphasis on video and radio signal processing.

**Milan Z. Bjelica** has received BSc and MSc degrees from the Faculty of Technical Sciences, University of Novi Sad, Serbia. He is currently employed as a software design engineer at RT-RK LLC, and as the teaching assistant at the University of Novi Sad. He is also working towards his PhD degree at the department for Computer Engineering and Computer Communications, at Faculty of Technical Sciences, Novi Sad. His research interests and expertise include novel immersive context-aware systems, usability assessment and home automation systems, frequently applied to the different consumer electronics devices.

**Dragan Kukolj** has received his Diploma degree in control engineering in 1982, MSc degree in computer engineering in 1988, and PhD degree in control engineering in 1993, all from the University of Novi Sad, Serbia. He is currently a Professor of computer-based systems with Department of Computing and Control, Faculty of Engineering, University of Novi Sad. His main research interests include soft computing, data mining techniques and computer-based systems integration with applications in video processing and digital signal processing. He has published over 100 papers in referred journals and conference proceedings. He is the coordinator of Intellectual Property Centre of Faculty of Engineering.

Bojan Mrazovac et al.

**Branislav M. Todorović** received his Dipl.Eng. and M.Sc. degrees from the Faculty of Electrical Engineering, University of Belgrade, Serbia and Ph.D. degree from the Faculty of Technical Sciences, University of Novi Sad, Serbia in 1983, 1988 and 1997, respectively. He is a Senior research fellow at the RT-RK, Institute for Computer Based Systems, and a Professor at the Military Academy, University of Defense, Belgrade. Prior to joining RT-RK, he was with the Institute of Microwave Techniques and Electronics (IMTEL), Centre for Multidisciplinary Research and the Military Technical Institute (VTI, Institute of Electrical Engineering) in Belgrade. His research interests are in the wide area of radio signals, telecommunications and digital signal processing. He has authored or coauthored about 100 referred journal and conference papers and two books. He is a Member of the IEEE and Fellow of the Institute of Nanotechnology (UK).

**Saša Vukosavljev** has received his BSc and MSc degree from the Faculty of Technical Sciences, University of Novi Sad, Serbia. He is currently employed as a senior embedded software developer in RT-RK, Institute for Computer Based System, Novi Sad. His main research interests include low power embedded real time systems, lightweight sensors, signal processing and autonomous robots. He took part in European competition in robotics in France in 2001 and 2002. He has authored and coauthored about 30 conference papers.

*Received: May 31, 2012; Accepted: November 12, 2012.*